

## **Corrosion Behavior of Alloy Structural Steels in Catechol and Biomass-Derived Pyrolysis Oils**

Jiheon Jun, Dino Sulejmanovic, James R. Keiser, Michael P. Brady and Michael D. Kass

Material Science and Technology Division, Oak Ridge National Laboratory,  
One Bethel Valley Road, Oak Ridge, TN 37831, USA

### **ABSTRACT**

Electrochemical impedance spectroscopy (EIS) was used to assess the corrosion behavior of three steels, 2.25Cr-1Mo, 5Cr-1Mo and 9Cr-1Mo (UNS K21590, S50200 and K90941) in bio-oils and catechol, an organic constituent commonly found in bio-oils. Two types of biomass pyrolysis oils produced from selected forest residue feedstocks, classified as high-ash and high-moisture (HAHM) and low-ash and low-moisture (LALM) types and 10 wt.% catechol, were used to test the alloys. According to previous results, 10 wt.% catechol in a water and methanol mixture was corrosive to 2.25Cr-1Mo but not to 9Cr-1Mo, highlighting that increasing Cr content in the steels resulted in improved corrosion resistance. 5Cr-1Mo, a steel with an intermediate Cr content, was tested in catechol solutions to better estimate the critical value of Cr for corrosion resistance under these conditions. Also, the three alloys were tested in both HAHM and LALM bio-oils to assess corrosion susceptibility. For EIS measurements, a customized electrochemical setup was employed to minimize the ohmic path through the bio-oils. The corrosion susceptibility was evaluated by determining the resistance at the alloy-corrosive medium interface.

**Key words:** biomass pyrolysis oil, structural steels, bio-oil storage, Electrochemical Impedance Spectroscopy, corrosion

### **INTRODUCTION**

Biomass-derived pyrolysis oil, a renewable energy source, has corrosivity originating from its water and organic acid contents.<sup>1-5</sup> For example, a plain carbon steel and 2.25Cr-1Mo steel suffered from severe pitting attack, causing some pits deeper than 500 µm, after 1000 h exposure to a pine sawdust bio-oil at 50°C.<sup>6</sup> To avoid corrosion attack by bio-oils, the use of stainless steels can be a practical, but expensive solution.

It was previously reported that mixed hardwood bio-oil exposure resulted in relatively small and essentially no corrosion mass loss for types 409 and 316L stainless steels (UNS S40900 and UNS S31603), respectively, as opposed to the greater mass losses measured in a plain carbon

and 2.25Cr-1Mo steel.<sup>7</sup> Lower or no mass loss of stainless steels was also observed in a similar study that used a different bio-oil.<sup>8</sup>

Besides the direct bio-oil exposure and corrosion loss measurements, electrochemical impedance spectroscopy (EIS) was used to evaluate the corrosion resistance of various ferrous alloys in selected constituents of bio-oils, i.e. formic acid, catechol and lactobionic acid.<sup>9-11</sup> Based on the resistance values determined from the impedance spectra, both 2.25Cr-1Mo and 9Cr-1Mo (UNS K21590 and K90941) steels were susceptible to corrosion in 10 wt.% formic and lactobionic acids, but in 10 wt.% catechol, 9Cr-1Mo steel exhibited a high resistance to corrosion reaction(s) whereas 2.25Cr-1Mo steel did not.<sup>11</sup> These results suggest that there is a critical Cr content in between 2.25 and 9 wt.% to achieve corrosion resistance in catechol solution.

It is important to compare the corrosion behavior of the alloys not only in bio-oil constituents but also in real bio-oils. To address this, three Cr-Mo alloyed steels with increasing Cr contents were tested in 10 wt.% catechol solution and two types of bio-oils to determine the corrosion resistance or susceptibility of each using EIS. To enable EIS measurements in low-conductivity bio-oils, a custom-designed electrochemical cell was utilized. With another concurrent paper,<sup>12</sup> this is one of the initial attempts where EIS measurements were directly made in raw bio-oils for the evaluation of alloy corrosion behavior.

## EXPERIMENTAL METHODS

The three alloys used in this work were 2.25Cr-1Mo, 5Cr-1Mo (UNS S50200) and 9Cr-1Mo steels with their measured or nominal compositions presented in Table 1. Disks with 16 mm diameter and 2-3 mm thickness were machined from each alloy. All alloy disks were finished with 600 grit, water-rinsed and dried prior to EIS measurements.

**Table 1**  
**Chemical composition of 2.25Cr-1Mo, 5Cr-1Mo and 9Cr-1Mo steels in mass percent, while N, O and S contents are in ppm. Inductively coupled plasma optical emission spectroscopy and combustion techniques were used for the composition analysis.**

Alloy	UNS No.	Fe	Cr	Ni	Mn	Mo	Cu	Si	C	N	O	S	Other
2.25Cr-1Mo	K21590	95.7	2.22	0.14	0.51	1.01	0.09	0.17	0.092	45	9	50	0.01Co
5Cr-1Mo*	S50200	94	5	-	-	1	-	-	-	-	-	-	-
9Cr-1Mo	K90941	88.4	9.08	0.09	0.56	0.99	0.03	0.61	0.07	-	-	50	0.08Co, 0.06V

\*nominal composition

The custom designed cell for EIS measurements is described in detail elsewhere.<sup>12</sup> In short, the basic principle is to place the working, counter and reference electrodes very close to each other to minimize ohmic drop. The alloy disks in a holder with a defined exposure area and platinum mesh were the working and counter electrodes, respectively. The exposed areas were 1 cm<sup>2</sup> for 2.25Cr-1Mo and 9Cr-1Mo steels and 0.58 cm<sup>2</sup> for 5Cr-1Mo steel. The reference mercury sulfate electrode (MSE) was used with a glass Luggin capillary filled with saturated K<sub>2</sub>SO<sub>4</sub>. 10 wt.% catechol solution was prepared using a mixture of 85 wt.% DI water and 15 wt.% ethanol as the

solvent. The catechol solution was kept in a closed container at room temperature over 60 days before use in order to allow the oxidation of catechol in the solution. After this storage period, it was considered that the catechol oxidation is mostly complete thereby not significantly changing the solution composition.

Two bio-oils derived from Low Ash Low Moisture (LALM) and High Ash High Moisture (HAHM) forest residue biomass were used for this work. These LALM and HAHM bio-oils were produced by the National Renewable Energy Laboratory (Golden, CO, USA), and their chemical and combustion properties can be found elsewhere.<sup>13</sup> The conductivities of LALM and HAHM oils, measured by a commercial conductivity meter, was  $\sim 30$  and  $\sim 120 \mu\text{S}\cdot\text{cm}^{-1}$ , respectively. These values are lower than the conductivity of common tap water,  $\sim 270 \mu\text{S}\cdot\text{cm}^{-1}$ . A photo of the assembled electrochemical cell filled with HAHM bio-oil is shown in Figure 1.

A sequence of corrosion potential ( $E_{\text{corr}}$ ) and EIS measurement steps was used multiple times per each steel specimen. The term *immersion time* is defined as the time for which an alloy was exposed in catechol solution or bio-oils prior to each EIS step. The first EIS measurement only counts the initial  $E_{\text{corr}}$  step as the immersion time, but the following EIS measurements take all the previous  $E_{\text{corr}}$  and EIS steps to determine the immersion time. EIS measurements were conducted using  $\pm 10 \text{ mV}$  with respect to  $E_{\text{corr}}$  and the frequencies from 200 kHz to 5 mHz. For the entire measurements, the catechol solution and bio-oils were open to air at room temperature. For each test, the volume of catechol or bio-oil (LALM or HAHM type) was approximately 100 mL.

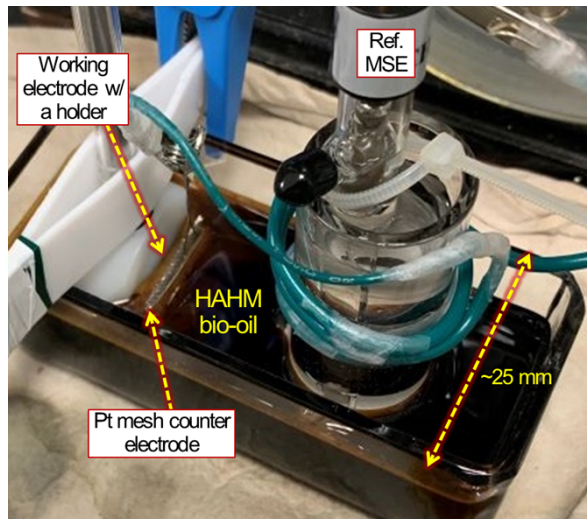


**Figure 1: A photo of electrochemical cell filled with HAHM bio-oil. The volume of bio-oil in the glass container was about 100 mL.**

## RESULTS

The impedance spectra of a 2.25Cr-1Mo steel specimen are shown in the  $Z'$  and  $Z''$  (real and imaginary impedances) plane in Figure 2 for 2 h and 19.5 h immersion times in 10 wt.% catechol and LALM bio-oil. On the left and right sides of the  $Z'$  axis, there are imperfect arcs and depressed semi-circles which correspond to the impedance responses of the electrolyte (bio-oil or 10 wt.%

catechol) and the corrosion reaction at the alloy interface, respectively, as previously noted.<sup>11</sup> The  $Z'$  width of the depressed semi-circles, i.e. the distance from each end, can be used to estimate the degree of corrosion reaction.<sup>11</sup> For 2.25Cr-1Mo steel, the  $Z'$  width did not notably change by increasing the immersion time for both catechol and bio-oil (~800 to ~1000 and ~1800 to ~2200  $\text{ohm}\cdot\text{cm}^2$ , respectively), implying that the corrosion reaction was relatively consistent over time. The impedance plots of 2.25Cr-1Mo in HAHM bio-oil were presented elsewhere<sup>12</sup> where the  $Z'$  width of the depressed semi-circle after an 18 h immersion was about 2000  $\text{ohm}\cdot\text{cm}^2$ , not significantly different from the width after a 19.5 h immersion in LALM bio-oil.

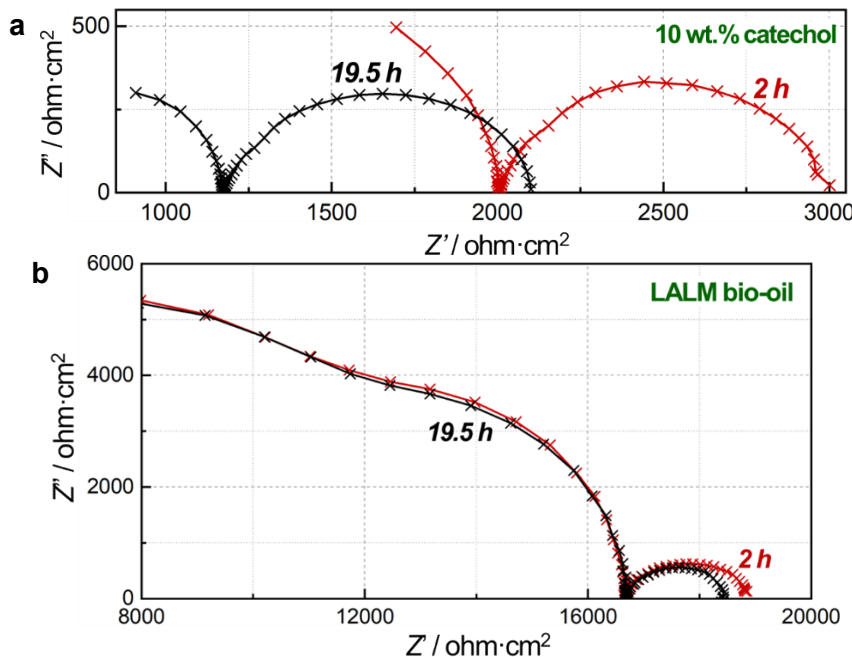


**Figure 2: Impedance spectra of 2.25Cr-1Mo steel in (a) 10 wt.% catechol and (b) LALM bio-oil for different immersion times. The impedance data in (a) are shown with the lowest frequency of 0.02 Hz because the impedance plot at lower frequencies was highly erratic. This irregular impedance plot was likely caused by a very low conductivity of 10 wt.% catechol solution ( $\sim 35 \mu\text{S}\cdot\text{cm}^{-1}$ )<sup>11</sup> and not useful to capture meaningful corrosion processes.**

Figure 3 shows the impedance spectra of 5Cr-1Mo steel in LALM and HAHM bio-oils as well as 10 wt.% catechol solution. In the catechol solution, there was a partial semi-circle after a 2 h immersion, with the  $Z'$  width larger than 5000  $\text{ohm}\cdot\text{cm}^2$ , and a smaller depressed semi-circle at 19.5 h, with the  $Z'$  width smaller than 2000  $\text{ohm}\cdot\text{cm}^2$  (designated by arrows on the right sides of the initial arcs in Fig. 3a). This could be indicative of a corrosion reaction that was somewhat slower in the beginning. The  $Z'$  width of depressed semi-circles, associated with the corrosion reaction, increased slightly with time in LALM and HAHM bio-oils but remained below 2000  $\text{ohm}\cdot\text{cm}^2$ . Except in one case (5Cr-1Mo in 10 wt.% catechol at 2 h immersion time), the magnitude of the  $Z'$  width in 2.25Cr-1Mo and 5Cr-1Mo steels did not show notable differences in all measurements.

The impedance spectra of 9Cr-1Mo steel are plotted in Figure 4 for different immersion times in the three corrosive media. In the catechol solution, 9Cr-1Mo steel exhibited increasing  $Z'$  and  $Z''$  values after the initial arcs ending at  $Z = \sim 2000$  and  $\sim 3000 \text{ ohm}\cdot\text{cm}^2$ . For the impedance portion associated with corrosion reactions, the  $Z''$  width values are approximated as greater than 20  $\text{kohm}\cdot\text{cm}^2$ , which implicates that 9Cr-1Mo was not susceptible to corrosion in the catechol solution. In LALM and HAHM bio-oils, inductive loops appeared before the depressed semi-circles. Again, any impedance response except the semi-circle portions are likely associated with the bio-oils and testing conditions that are not the main focus of this work. The  $Z''$  width values of 9Cr-1Mo in the bio-oils were smaller than 1000  $\text{ohm}\cdot\text{cm}^2$ .

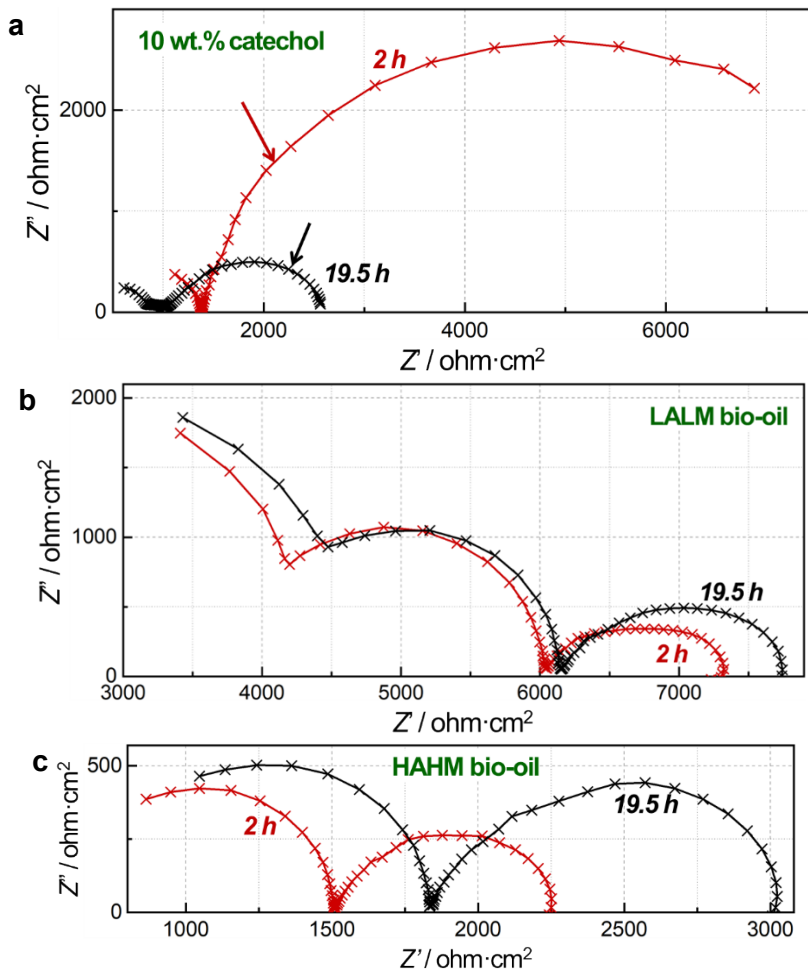


**Figure 3: Impedance spectra of 5Cr-1Mo steel in (a) 10 wt.% catechol and (b, c) LALM and HAHM bio-oils for different immersion times. The impedance data in (a) are shown with the lowest frequency of 0.07 and 0.016 Hz for 2 h and 19.5 h measurements, respectively.**

The resistance to corrosion reaction ( $R_2$ ), or more generally the charge transfer resistance, was determined from fitting the EIS data using a simple equivalent circuit. Note that all EIS data presented in this work had chi-squire smaller than 0.001. The  $R_2$  values of the three Cr-Mo alloyed steels in 10 wt.% catechol are plotted as a function of immersion time in Figure 5 with an inset figure showing the equivalent circuit used for the EIS data fitting. A method of EIS fitting used in

this work was previously described.<sup>11</sup> The 2.25Cr-1Mo and 5Cr-1Mo steel specimens exhibited  $R_2$  values decreasing with time and became lower than 2500  $\text{ohm}\cdot\text{cm}^2$  while the  $R_2$  values for 9Cr-1Mo were greater than 13  $\text{kohm}\cdot\text{cm}^2$  in all cases.

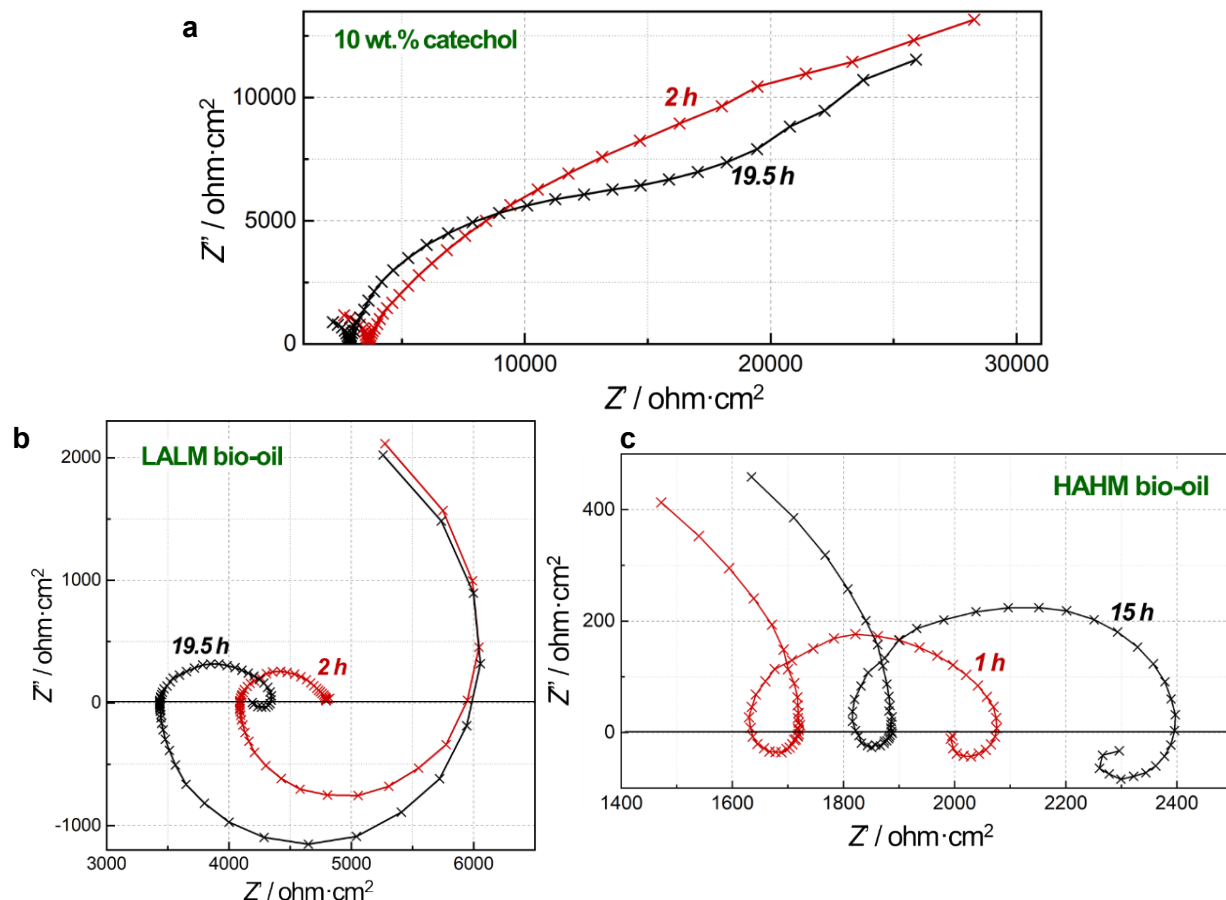


**Figure 4: Impedance spectra of 9Cr-1Mo steel in (a) 10 wt.% catechol and (b, c) LALM and HAHM bio-oils for different immersion times.**

In a previous report, the  $R_2$  values of actively corroding carbon steel and ductile iron were 2500~3700  $\text{ohm}\cdot\text{cm}^2$  as determined by EIS data fitting.<sup>14</sup> This supports the conclusion that 2.25Cr-1Mo and 5Cr-1Mo steels with  $R_2 < 2500 \text{ ohm}\cdot\text{cm}^2$  were susceptible to corrosion in 10 wt.% catechol. Meanwhile, the 9Cr-1Mo steel specimen with a higher  $R_2$  value could be considered less susceptible or relatively resistant to corrosion. Note that a recent EIS measurement also reported low and high  $R_2$  values of 2.25Cr-1Mo and 9Cr-1Mo steels (< 1 and >100  $\text{kohm}\cdot\text{cm}^2$ , respectively) in a very similar 10 wt.% catechol solution (where the solvent was 85 wt.% DI water and 15 wt.% methanol).<sup>11</sup> Taking the  $R_2$  results into account, the critical Cr content to resist catechol should be greater than 5 wt.% but slightly lower or close to 9 wt.% Cr.

The  $R_2$  values of the steels in LALM and HAHM bio-oils are presented in Figure 6 and 7, respectively, as a function of immersion time. All the steels exhibited low  $R_2$  values, less than 3100  $\text{ohm}\cdot\text{cm}^2$ , indicating that they were not resistant to corrosion in both LALM and HAHM bio-oils. Note that the  $R_2$  for 2.25Cr-1Mo steel in HAHM bio-oil was also relatively low, less than 4000  $\text{ohm}\cdot\text{cm}^2$ , as reported elsewhere.<sup>12</sup> The post-exposure surfaces of the steels are shown in Figure

8. The 9Cr-1Mo steel specimen after 10 wt.% catechol exposure was the only case with no visual change on the surface. These results agree with the  $R_2$  comparison results where 9Cr-1Mo steel in 10 wt.% catechol was assessed relatively corrosion-resistant but the other steels are more susceptible to corrosion. Based on the results presented here, none of the Cr-Mo alloyed steels is expected to be compatible with commercial bio-oils. For corrosion compatibility in bio-oils, stainless steel grades with higher Cr contents should be considered.

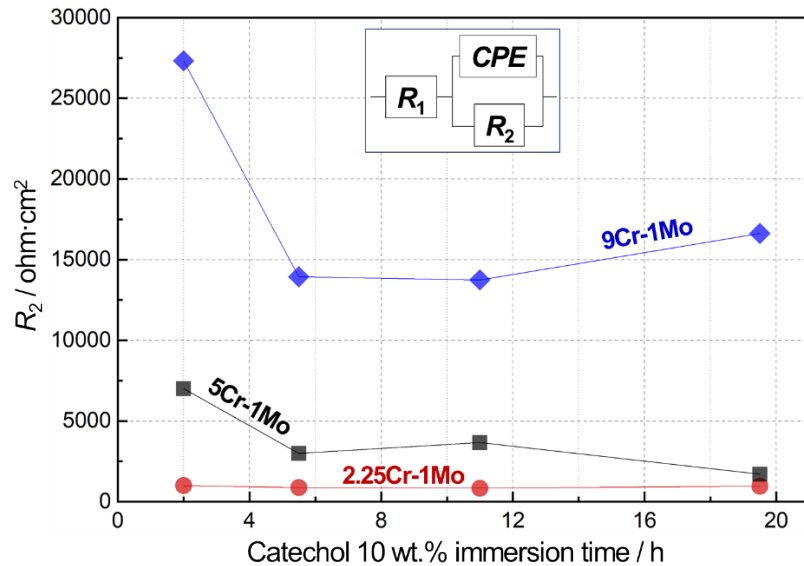


**Figure 5:  $R_2$  of Cr-Mo steels in 10 wt.% catechol as a function of immersion time. The inset figure shows the equivalent circuit used for EIS data fitting.  $R_1$  is the bulk electrolyte resistance, and constant phase element (CPE) accounts for non-ideal capacitive behavior at the interface of steel and electrolyte.**

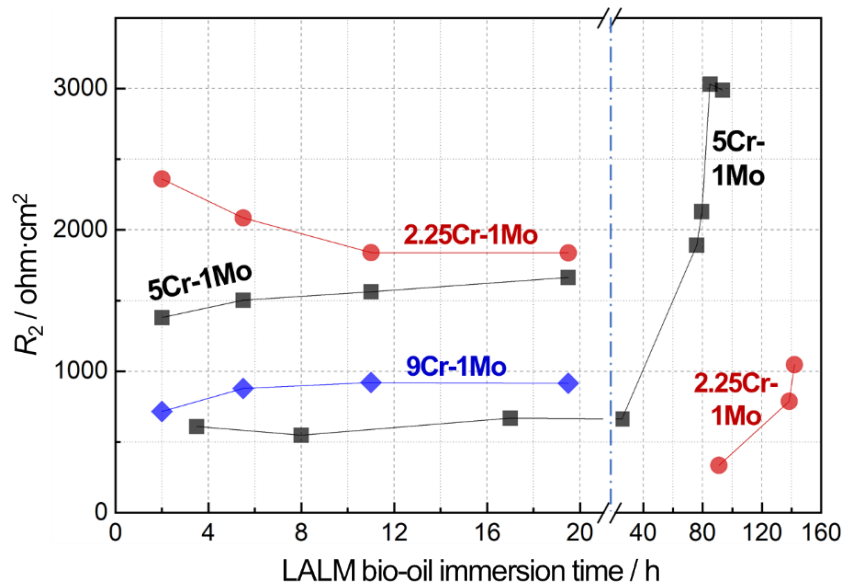


**Figure 6:  $R_2$  of Cr-Mo steels in LALM bio-oil as a function of immersion time. Two independent measurements were measured for 2.25Cr-1Mo and 5Cr-1Mo steels.**

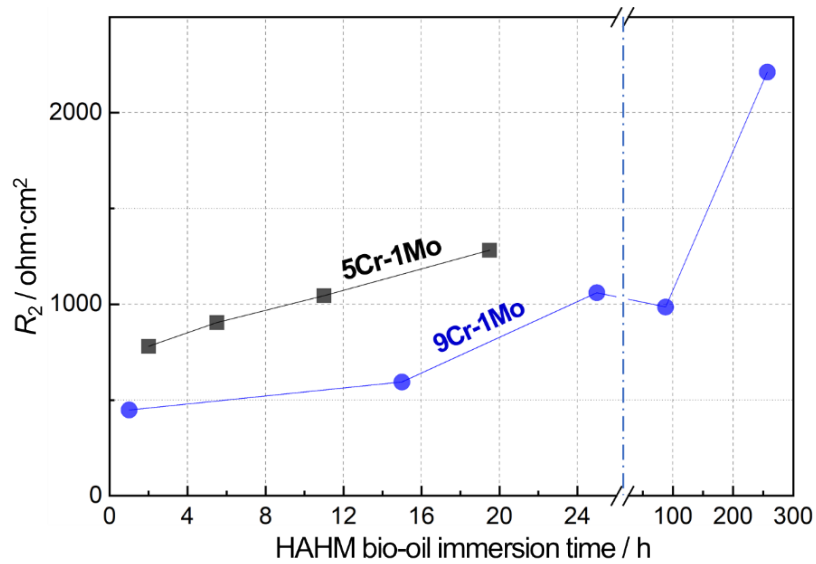


Figure 7:  $R_2$  of 5Cr-1Mo and 9Cr-1Mo steels in HAHM bio-oil as a function of immersion time.  $R_2$  of 2.25Cr-Mo steel in HAHM bio-oil is presented elsewhere.<sup>12</sup>

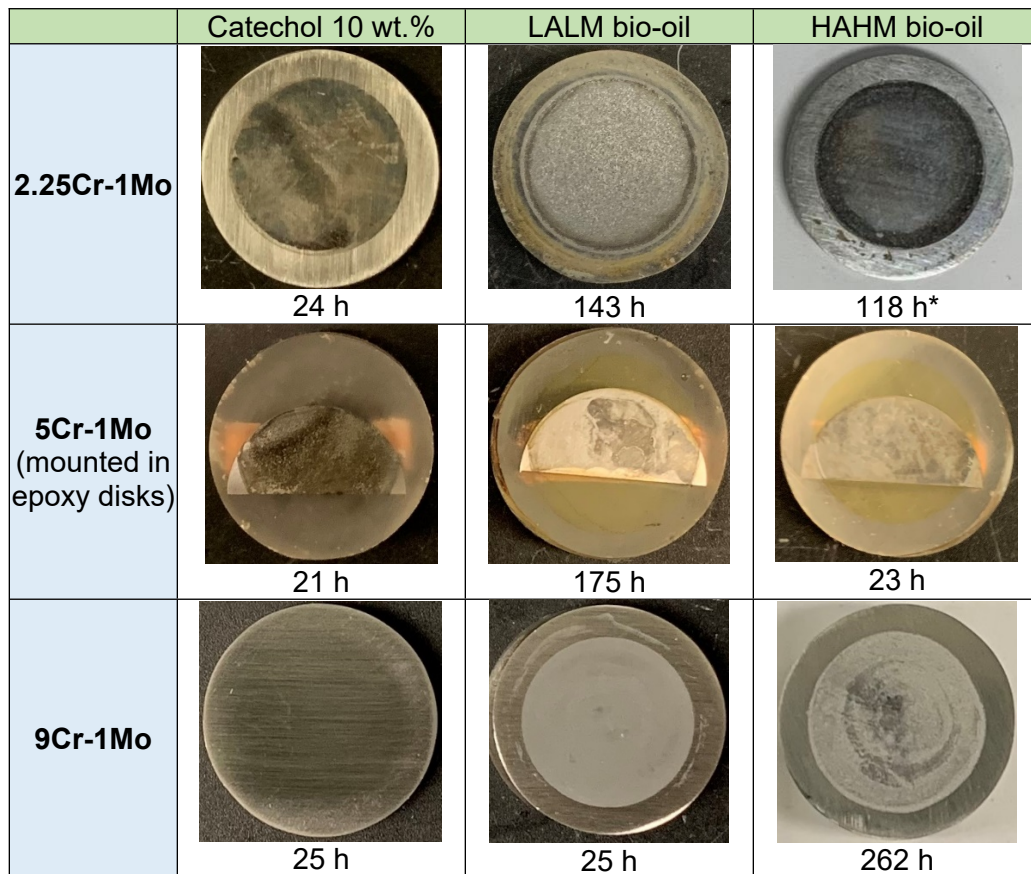


Figure 8: Post-exposure surfaces of Cr-Mo steels after EIS measurements in 10 wt.% catechol and the two bio-oils. The diameters of 2.25Cr-1Mo and 9Cr-1Mo disks and epoxy disks with 5Cr-1Mo are 16 mm. \*Also presented in another reference<sup>12</sup>

## CONCLUSION

The corrosion susceptibility of three Cr-Mo steels were evaluated using EIS in 10 wt.% catechol solution and LALM and HAHM bio-oils. The  $R_2$  values, the resistance to corrosion reaction, were determined from impedance spectra fitting. The  $R_2$  value for 9Cr-1Mo in 10 wt.% catechol was over 13 kohm·cm<sup>2</sup> with no visual change in the post-exposure surface, indicating that the steel was resistant to corrosion. However, in LALM and HAHM bio-oils, 9Cr-1Mo exhibited relatively lower  $R_2$  values with visually changed surfaces, evidencing its corrosion susceptibility to the bio-oils. The 2.25Cr-1Mo and 5Cr-1Mo steels were susceptible to corrosion in all test conditions with relatively low  $R_2$  values and corroded/reacted surfaces. With the  $R_2$  results presented here, the critical Cr content for catechol resistance must be greater than 5 wt.% but less than 9 wt.%.

## ACKNOWLEDGEMENTS

Funding for this research was provided by the U.S. Department of Energy, Office of Energy and Renewable Energy, Bioenergy Technologies Office. Sebastien Dryepondt, Xin He and Bruce Pint at ORNL provided helpful comments on the manuscript. This research was sponsored by the U.S. Department of Energy, Bioenergy Technologies Office. This manuscript has been authored by UT-Battelle, LLC under Contract No. DE-AC05-00OR22725 with the U.S. Department of Energy. The United States Government retains and the publisher, by accepting the article for publication, acknowledges that the United States Government retains a non-exclusive, paid-up, irrevocable, world-wide license to publish or reproduce the published form of this manuscript, or allow others to do so, for United States Government purposes. The Department of Energy will provide public access to these results of federally sponsored research in accordance with the DOE Public Access Plan (<http://energy.gov/downloads/doe-public-access-plan>).

## REFERENCES

1. S. Czernik and A. V. Bridgwater, "Overview of Applications of Biomass Fast Pyrolysis Oil", *Energy & Fuels* 18, 2 (2004) pp. 590-598.
2. D. C. Elliott, "Historical Developments in Hydroprocessing Bio-oils", *Energy & Fuels* 21, 3 (2007) pp. 1792-1815.
3. G. Huber and A. Corma, "Synergies between Bio- and Oil Refineries for the Production of Fuels from Biomass", *Angewandte Chemie International* 46, 38 (2007) pp. 7184-7201.
4. M. P. Brady, J. R. Keiser, D. N. Leonard, L. Whitmer and J. K. Thomson, "Corrosion Considerations for Thermochemical Biomass Liquefaction Process Systems in Biofuel Production", *JOM* 66 (2014) pp. 2583-2592.
5. M. D. Kass, B. L. Armstrong, B. C. Kaul, R. M. Connatser, S. A. Lewis, J. R. Keiser, J. Jun, G. Warrington, and D. Sulejmanovic, "Stability, Combustion, and Compatibility of High-Viscosity Heavy Fuel Oil Blends with a Fast Pyrolysis Bio-Oil", *Energy Fuels* 34, 7 (2020) pp. 8403-8413.

6. J. R. Keiser, M. P. Brady, R. M. Connatser, S. A. Lewis, "DEGRADATION OF STRUCTURAL ALLOYS IN BIOMASS-DERIVED PYROLYSIS OIL", Journal of Science & Technology for Forest Products and Processes 3, 3 (2013) pp. 16-22.
7. J. R. Keiser, M. Howell, S. A. Lewis, R. M. Connatser, "Corrosion Studies Of Raw And Treated Biomass-Derived Pyrolysis Oils". CORROSION 2012, Paper No. 1645 (Salt Lake City, UT: NACE, 2012).
8. J. R. Keiser, M. P. Brady, J. K. Thomson, R. M. Connatser, S. A. Lewis, and D. N. Leonard, "Bio-Oil Properties and Effects on Containment Materials". CORROSION 2014, Paper No. 4423 (San Antonio, TX: NACE, 2014).
9. J. Jun, M. G. Frith, R. M. Connatser, J. R. Keiser, M. P. Brady and S. A. Lewis, "Corrosion of Ferrous Alloys by Organic Compounds in Simulated Bio-Oils", CORROSION 2019, Paper No. 12895 (Nashville, TN: NACE, 2019).
10. R. M. Connatser, M. G. Frith, J. Jun, S. A. Lewis, M. P. Brady and J. R. Keiser, "Approaches to Investigate the Role of Chelation in the Corrosivity of Biomass-Derived Oils", Biomass & Bioenergy 133 (2020) p. 105446.
11. J. Jun, M. G. Frith, R. M. Connatser, J. R. Keiser, M. P. Brady and S. A. Lewis, "Corrosion Susceptibility of Cr-Mo Steels and Ferritic Stainless Steels in Biomass-Derived Pyrolysis Oil Constituents", Energy Fuels (2020) pp. 6220-6228.
12. J. Jun, D. Sulejmanovic, J. R. Keiser, M. P. Brady and M. D. Kass, "Evaluation of Corrosion Susceptibility of Structural Steels in Biomass Derived Pyrolysis Oil", CORROSION 2021, Paper No. 16502 (Salt Lake City, UT: NACE, 2021).
13. J. Klinger, D. L. Carpenter, V. S. Thompson, N. Yancey, R. M. Emerson, K. R. Gaston, K. Smith, M. Thorson, H. Wang, D. M. Santosa and I. Kutnyakov, "Pilot Plant Reliability Metrics for Grinding and Fast Pyrolysis of Woody Residues", ACS Sustainable Chem. Eng. 8 (2020) pp. 2793-2805.
14. J. Jun et al., "Methodologies for Evaluation of Corrosion Protection for Ductile Iron Pipe", ORNL/TM-2017/144 (2019) United States.